Polynomial Spline Surfaces with Rational Linear Transitions

Jörg Peters, Martin Sarov,
University of Florida

Abstract

We explore a class of polynomial tensor-product spline surfaces on 3-6 polyhedra, whose vertices have valence $n = 3$ or $n = 6$. This restriction makes it possible to exclusively use rational linear transition maps between the pieces: transitions between the bi-cubic tensor-product spline pieces are either C^1 or they are G^1 (tangent continuous) based on one single rational linear reparameterization. The simplicity of the transition functions yields simple formulas for a hierarchy of splines on subdivided 3-6 polyhedra.

Keywords: rational linear reparameterization, geometric continuity, genus, 3-6 polyhedra, pairs of pants, tensor-product splines, multi-resolution

1. Introduction

For genus $g = 1$, e.g. the torus, an affine atlas can be constructed, for example, using B-splines on a tensor-product grid, made periodic by setting equal the opposing edges. For genus $g > 1$, as a consequence of the Gauss-Bonnet Theorem, a closed, orientable, smooth 2-manifold does not have an affine atlas However, a paper in this conference series, [PF10], showed that there is a *rational linear reparameterization* for constructing smooth surfaces of genus $g > 0$ from tensor-product splines. If the reparameterization is structurally symmetric, i.e. indexing does not matter (cf. Definition 4), then it is unique.

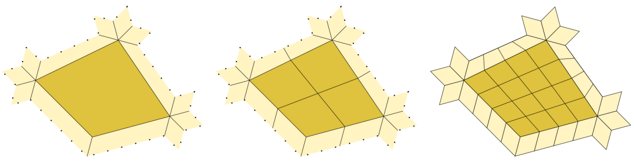

(a) a 3-6 quad (b) level $\ell = 1$ (c) level $\ell = 2$

Figure 1: (a) An example 3-6 quad with valences $n = 3, 6, 6, 6$ and its uniform binary subdivisions (b) at level $\ell = 1$ and (c) t level $\ell = 2$. Each (subdivided) 3-6 quad is associated with one tensor-product spline patch.

Together with Lemma 4 of [PF09], exclusive use of a structurally symmetric rational linear reparameterization implies that the resulting piecewise tensor-product spline surfaces must be assembled from basic pieces with the *restricted layout*: wherever the spline patches join with purely geometric continuity (G^1 continuity, not C^1 continuity) across a boundary, its end vertices must have equal valence.

By the 'hairy ball' theorem (see e.g. [EG79]), a regular surface of genus $g > 1$ must have transitions with purely geometric continuity. The paper [PF10] derived the apparently unique restricted layout for quad-only polyhedra: every quad has vertices of valence 8 or is a grid-like refinement thereof. This paper now presents a second, more natural family of restricted-layout quadrilateral polyhedra that uses less dramatic valences, namely any combination of $n = 3$ and $n = 6$ or a grid-like refinement of the quads (see Fig. 1).

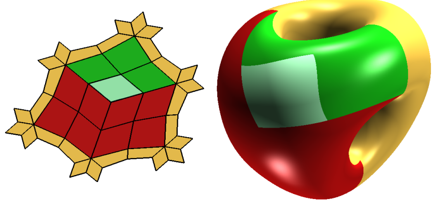

(a) 3-neighborhood, level 1 [3,6,6,6] quads, genus $g = 2$

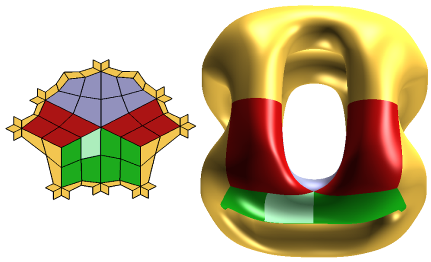

(b) 6-neighborhood, level 1 [3,6,6,6] quads, genus $g = 5$

Figure 2: The layout induced by once-subdivided 3-6 quads allows modelling smooth objects of any genus greater than one using one bi-cubic polynomial piece per sub-quad (a) uses 2×6 quads, (b) 8×6 quads.

The contributions of this paper are as follows.

- We exhibit a family of quadrilateral polyhedra, the 3-6 polyhedra, with vertices of valence $n = 3$ or $n = 6$, that satisfy the restricted layout. (Grid-like partition of the 3-6 quads of the 3-6 polyhedron yields additional vertices of valence $n = 4$, see Fig. 1, 2).
- The simplicity of the transition functions yields simple for-

mulas for a hierarchy of splines on grid-like subdivided input meshes. Each finer level offers additional geometric degrees of freedom (see Fig. 3) for detailed models.

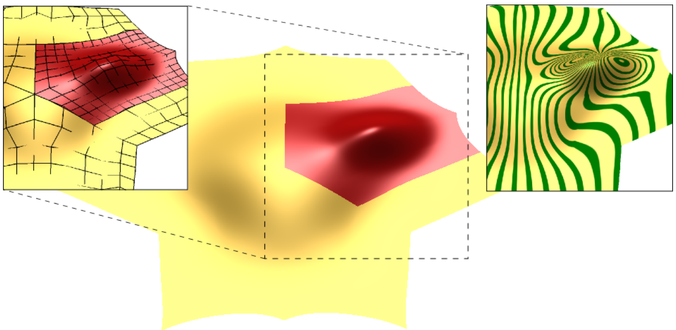

(a) Coarse basic function with fine addition

(b) Level $\ell = 1$ basic function + level $\ell = 2$ basic function = hierarchical edit

Figure 3: The simplicity of the transition functions yields simple formulas for a hierarchy of splines on subdivided input meshes. Basic, B-spline-like functions are associated with each vertex of the input control net. (a) A level $\ell = 1$ (coarse) basic function, located at a 6-valent vertex, is shown in gold. A fine basic function (at level $\ell = 2$) is added to create a combined (red) function that is smooth also across the 6-6 edge connecting two vertices of valence $n = 6$. The lower right inset displays highlight lines on the multi-level surface.

Overview. Section 2 reviews the pertinent literature. Section 3 formalizes the notion of a 3-6 polyhedron, their refinement and properties, the notion of structurally symmetric geometric continuity and explains the structure of the resulting surfaces. Section 4 introduces a hierarchy of G^1 spline surfaces on subdivided 3-6 polyhedrons, by providing a concrete algorithm and proving geometric continuity.

2. Literature

Since regular, differentiable 2-manifolds (surfaces) of genus $g \geq 2$ without boundary do not have an affine atlas, we cannot hope to just make an affine change of variables to transition between the tensor-product spline pieces of a regularly parameterized smooth closed surface of genus $g > 1$ in $\mathbb{R}^3$. However, if we allow rational linear reparameterization, we can, in principle, find conformal bijective orientation-preserving transition maps such as Möbius transformations. Concretely, [PF10] exhibited a unique rational linear reparameterization that allows structurally symmetric construction of smooth surfaces of genus $g > 0$. This reparameterization relates the derivatives of two abutting spline patches p and q along their common curve by *linear scaling*, i.e.

$$\partial_2 p(t, 0) + \partial_2 q(0, t) = \omega(t)\partial_1 p(t, 0) \qquad \text{(G1)}$$

where $\omega(t)$ is linear.

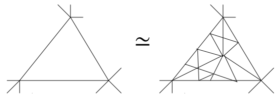

(a) base triangle triangulated

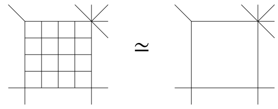

(b) 3-6 quad and its subdivision

Figure 4: Reduction to the base structure.

An independent result, [PF09, Lemma 4], rules out general G^1 constructions with $\omega(t)$ linear everywhere with one exception: the derivatives can be everywhere related by (G1) if the endpoints $p(0, 0)$ and $p(1, 0)$ have the same valence – or if ω in (G1) is constant. In short, 'linearly $G1$-connected vertices must have the same valence'.

More recently, Beccari et al. [BGN14] introduced RAGS, a construction using *rational three-sided macro* patches connected by a rational linear reparameterization (whereas the four-sided patches in [PF10] are *polynomial*). This approach generalizes the work of Alfeld, Neamtu and Schumaker, who obtained functions on surfaces by restricting trivariate polynomials to a genus $g = 0$ surface [ANS96] and credited part of their approach to [Möb46]. Pottmann and Wallner applied hyperbolic geometry to model smooth surfaces of higher genus by rational splines [WP98] and [VJK08] used the classical Möbius map to assemble an atlas from overlapping disks. Atlas-based surface construction was pioneered by [GH95].

While [BGN14] proposes a computation to enforce constraints that allow for a rational linear reparameterization, a careful reading of [BGN14] shows that, in the *structurally symmetric* case, their construction uses the rational linear reparameterization derived in [PF10] for three-sided patches – an observation that uniqueness of the parameterization up to a scalar degree of freedom already predict. Once a structurally symmetric base atlas of three-sided patches has been created, each three-sided patch can be irregularly partitioned into triangular macro-patches and additional vertices resulting from splitting triangles can have any number of neighbors (see Fig. 4a). It is only after pruning away these extra triangulations that the underlying structure becomes apparent and shows that structurally symmetric G^1 constructions are equally restricted for triangular patches as for tensor-product patches.

3. Restricted quad-layouts compatible with rational linear transition maps

Below, in Section 3.1, we define the restricted patch layout and a class of polyhedra, the 3-6 polyhedra, that can be endowed with a piecewise tensor-product spline surface to satisfy a restricted patch layout. In Section 3.2 we review the definition of and results concerning the geometric continuity of structurally symmetric rational linear transition maps. Finally, in Section 3.3, we show how we index the tensor-product patches and their coefficients.

3.1. Restricted quad-layout and 3-6 polyhedron

Euler's formula, $v - e + f = \chi$, characterizes closed polyhedra by relating the numbers of vertices v, edges e and faces f of

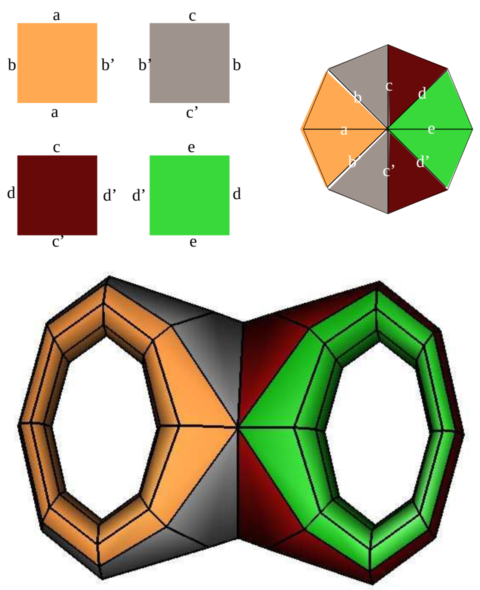

Figure 5: Figure-8 (from [PF10]): *left*: Identification of edges of the 4 quadrilaterals. *middle*: Embedding in $\mathbb{R}^3$ with $2g - 2 = 2$ corner points of valence 8. *right*: Corresponding smooth spline surface with central saddle shape.

a given polyhedron to the Euler characteristic (Euler-Poincaré characteristic) $\chi = 2 - 2g$. Here g is the topological genus, i.e. the number of handles. For example, Fig. 2b shows a surface of genus 5 built exclusively from quads whose vertices have valence $n = 3, 6, 6$ and 6. We note that since we can associate with each 4-valent vertex four half-edges and four quarters of attached quads the net contribution of 4-valent vertices to the Euler count is $1 - 4/2 + 4/4 = 0$. Then adding or removing checkerboard arrangements of quadrilaterals does not affect the left hand side $v - e + f$ of Euler's formula (cf. Fig. 4b).

Lemma 4 of [PF09] proves that structurally symmetric geometrically smooth surfaces constructions must relate some abutting patches with quadratic or higher-degree reparameterizations – unless they have a restricted layout. Restricted layout relates the smoothness of the surface to the underlying (polyhedral) layout of the patches as follows.

Definition 1 (restricted patch layout). *A surface has* restricted patch layout *if, wherever two vertices are connected by a curve across which two splines match according to (G1) with ω linear and not constant, the vertices have an equal number of neighbors.*

Note that the two splines in Definition 1 may consist of multiple polynomial pieces.

[PF10] showed that restricted patch layouts exist and presented a construction of spline surfaces on partitions consisting exclusively of quadrilaterals all of whose corner vertices are 8-valent (see Fig. 5; to obtain additional geometric degrees of freedom without affecting the Euler count, quadrilaterals can be partitioned). At the time, this base layout appeared to be only quad-layout yielding a restricted patch layout.

[PF10] also proved that the projective linear (rational linear) reparameterization for constructing smooth surfaces of genus $g > 0$ from tensor-product splines is essentially unique and results in a linear relation of derivatives for adjacent patches. Together with Lemma 4 of [PF09] this implies that constructing manifolds with a rational linear reparameterization requires a restricted layout of the quadrilaterals that is achieved by the following.

Definition 2. (3-6 quad, 3-6 polyhedron, restricted polyhedron) *A* 3-6 quad *is a quadrilateral facet whose vertices have valence $n = 3$ or $n = 6$. The edges of a 3-6 quad are called* 3-3 edge, 3-6 edge *or* 6-6 edge *according to the valence of the endpoints. A polyhedron is a* 3-6 polyhedron *if it consist entirely of 3-6 quads. A polyhedron is a* restricted polyhedron *if it can be obtained from a 3-6 polyhedron by splitting its 3-6 quads.*

In the following, we will split 3-6 quads only in a uniform, binary fashion and the 3-6 polyhedron is endowed with a surface construction that satisfies the restricted patch layout by relating constantly the derivatives of patches abutting across curves connecting vertices of valence 3 and valence 6 (6-3 edges or 3-6 edges) and linearly across 3-3 edges and 6-6 edges. However other partitions may be useful for practical and artistic purposes [HXA+12, Akl14].

A 3-6 quad with n_3 vertices of valence $n = 3$ contributes $(n_3 - 2)/6$ to the $v - e + f$ count of Euler's formula. For example, using exclusively 3-6 quads with a single vertex of valence $n = 3$, Fig. 2a consists of 12 once-subdivided 3-6 quads that have 4 vertices of valence 3 and 6 vertices of valence 6. Fig. 2b consists of 48 once-subdivided 3-6 quads that have 16 vertices of valence 3 (two per cube corner, one inside, one outside) and 24 vertices of valence 6 (two per cube edge).

3.2. Geometric continuity of structurally symmetric rational linear transition maps

While the smoothness of the resulting surface can be expressed in the language of differential geometry, i.e. in terms of overlapping charts (see e.g. the construction in [YZ04]) it suffices, and is often more efficient, to express smoothness as agreement of one-sided jets, i.e. equivalence classes of Taylor expansions, along the curve where two surface pieces are glued together. We use this approach in the following.

Definition 3 (geometric continuity, G^1). *Two surface pieces $\mathbb{c}^\alpha$ and $\mathbb{c}^\beta$ that join along a curve $\gamma(t) := \mathbb{c}^\alpha(t, 0) = \mathbb{c}^\beta(0, t)$ join G^1 if there exists a suitably oriented and non-singular reparameterization $\rho : \mathbb{R}^2 \to \mathbb{R}^2$, so that the jets $\partial^k \mathbb{c}^\alpha$ and $\partial^k(\mathbb{c}^\beta \circ \rho)$, agree at every point $\gamma(t)$ for $k = 1$.*

That is, adjacent surface pieces are related by reparameterization ρ, so that, up to first order, $\mathbb{c}^\alpha = \mathbb{c}^\beta \circ \rho$. Although ρ is just a change of variables, its choice is crucial for the properties of the surface.

Definition 4 (structurally symmetric reparameterization). *A reparameterization $\rho : \mathbb{R}^2 \to \mathbb{R}^2$ and the corresponding G^1 surface construction is* structurally symmetric *(or* unbiased*) if both $\partial \mathbb{c}^\alpha = \partial(\mathbb{c}^\beta \circ \rho)$ and $\partial \mathbb{c}^\beta = \partial(\mathbb{c}^\alpha \circ \rho)$.*

[PF10] showed that a structurally symmetric G^k transition with a rational linear reparameterization must have the form

$$\partial^i(\mathbb{c}^\alpha \circ r^\alpha_{\mathbb{c}})(t,0) = \partial^i(\mathbb{c}^\beta \circ r^\beta_{\mathbb{c}})(t,0), \quad i = 0,\dots,k,$$
$$r^\alpha_{\mathbb{c}}(u,v) := \frac{1}{\mathsf{s}_0 + \eta v}\begin{bmatrix} -v \\ \mathsf{s}u + \mathsf{c}_0 v\end{bmatrix}, \quad r^\beta_{\mathbb{c}}(u,v) := \frac{1}{\mathsf{s}_0 - \eta v}\begin{bmatrix} \mathsf{s}_0 u - \mathsf{c}_0 v \\ v\end{bmatrix},$$
$$\mathsf{c}_0 := \cos\frac{2\pi}{n_0},\ \mathsf{s}_0 := \sin\frac{2\pi}{n_0}, \mathsf{c}_1 := \cos\frac{2\pi}{n_1},\ \mathsf{s}_1 := \sin\frac{2\pi}{n_1},$$

where n_0 is the valence at $\mathbb{c}^\alpha(0,0)$ and $\eta \in \mathbb{R}$ is determined by the valence n_1 at $\mathbb{c}^\alpha(1,0)$. Alternatively,

$$\rho(u,v) := r_{\mathbb{c}^\alpha} \circ r^{-1}_{\mathbb{c}^\beta} = \frac{1}{1 + 2v(\mathsf{c}_0 + \mathsf{c}_1)}\begin{bmatrix} -v \\ u + 2\mathsf{c}_0 v\end{bmatrix}.$$

connects the domains to form a common domain across the pre-image of $\gamma(t)$ and composition up to valence n many maps of type $r^\alpha_{\mathbb{c}}$ define a common pre-image or chart of the patches surrounding a vertex. We note that $\mathbb{c}^\alpha$ and $\mathbb{c}^\beta$ share $\gamma(t)$ and hence the derivatives along the common edge agree: $\partial_1\mathbb{c}^\alpha(t,0) = \partial_1\mathbb{c}^\beta(0,t)$. We need only check that, for a linear function $\omega(t)$, the partial derivative in the second direction match:

$$\partial_2\mathbb{c}^\alpha(t,0) + \partial_2\mathbb{c}^\beta(0,t) = \omega(t)\partial_1\mathbb{c}^\alpha(t,0). \qquad \text{(G1)}$$

The rational linear reparameterization implies that $\omega(t)$ which equals a partial derivative of the second coordinate is linear: $\omega(t) := \partial_2\rho^{[2]}(t,0) = (1-t)2\mathsf{c}_0 + t2(-\mathsf{c}_1)$. In particular, when $n_0 = 3$ and $n_1 = 6$ then $\omega(t) = 1$, i.e. the patch derivatives are in a constant relation and the patches are joined parametrically C^1.

To link the 3-6 polyhedron to a surface construction, we use the notion of *pair of pants*, or short pants. A pair of pants is a two-sphere with three open disks removed (see Fig. 6a,b). We provide concrete rational linear atlases for 3-6 polyhedra built from pants. Fig. 6d shows a smooth surface derived from one type of pants.

Lemma 1. *For any genus $g > 1$, 3-6 quads can form a 3-6 polyhedron and, by partition, a restricted polyhedron, that admits a smooth piecewise tensor-product spline surface satisfying a restricted patch layout.*

Proof Fig. 6 illustrates the fact that we can arrange (once subdivided) 3-6 quads into a basic building block that models a pair of (topological) pants Fig. 6b, i.e. two hexagonal fundamental polygons stitched together at every other side. It is well-known from hyperbolic geometry, that pairs of pants can be sewn together at their openings to create Riemann surfaces of any prescribed genus. The algorithm in Section 4.2 constructively shows that the resulting restricted polyhedron admits a smooth piecewise tensor-product spline surface according to (G1) and $\omega = 1$ for 3-6 edges and with one polynomial piece corresponding to each quad of the restricted polyhedron. |||

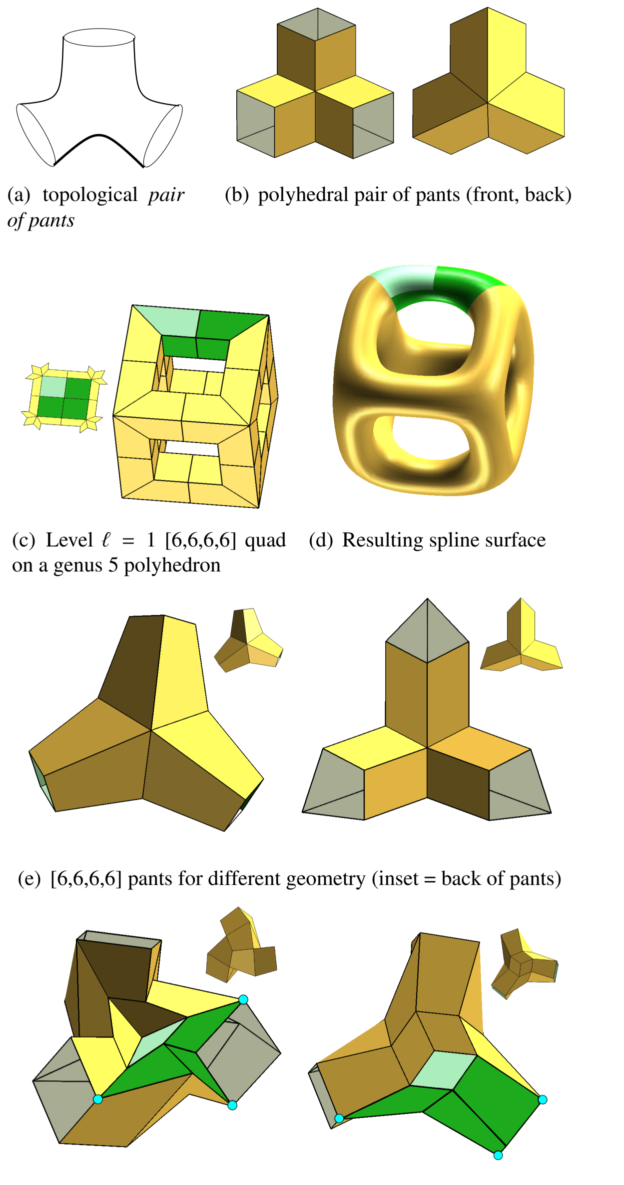

(a) topological *pair of pants* (b) polyhedral pair of pants (front, back)

(c) Level $\ell = 1$ [6,6,6,6] quad on a genus 5 polyhedron (d) Resulting spline surface

(e) [6,6,6,6] pants for different geometry (inset = back of pants)

(f) Two geometrically different [3,6,6,6] pants (inset = back)

Figure 6: The basic building block (a) a "pair of pants" can be modeled for example by (b) halves of level $\ell = 1$ [6,6,6,6] quads. (c) The pairs of pants combine to form a surface of genus 5 such that each [6,6,6,6] quad is shared by two pairs of pants and forms one half of a connecting tube. (The vertices are alternatingly 'inner' and 'outer' 6-valent vertices of the genus 5 polyhedron.) (d) The algorithm in Section 4 turns the 3-6 polyhedron into a smooth tensor-product spline surface with rational linear reparameterization. (e) Two geometrically different layouts of [6,6,6,6] pants yield the two spline surfaces of Fig. 12c. (f) Alternatively, pairs of pants can be constructed using [3,6,6,6] quads. For each geometrically different 3-6 polyhedron, one 3-6 quad of level $\ell = 1$ is colored as in (c) and in Fig. 2. Additionally, the vertices of valence 6 on the boundary of the pants are marked by a cyan-colored sphere. Unlike the [6,6,6,6] quads, the [3,6,6,6] quads are not shared between pants. The pants (f)*left*, with its three legs open (grey interior) towards the viewer, yields Fig. 12b, *left*. The pants (f)*right* yields a shape akin to Fig. 12c,*left*.

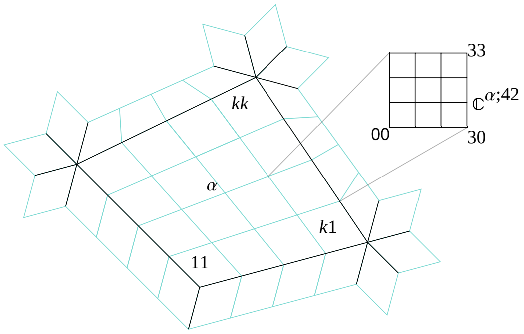

Figure 7: Partition of a 3-6 quad and the BB-net associated with one sub-quad.

3.3. *Indexing the surface pieces*

One of the nice properties of subdivision surfaces is that their refinement rules require only knowledge of the immediate neighborhood. By contrast, the hierarchical G^1 construction requires knowing the position within each 3-6 quad – at least along the 3-3 edges and the 6-6 edges. For simplicity of exposition, we choose this partition to be uniform and binary so that the partition at hierarchy level ℓ yields $2^\ell \times 2^\ell$ sub-quads indexed by the superscript $(k, l) \in 1 : 2^\ell$ (see Fig. 7).

Working locally, at a corner point of valence $n = 3$ or $n = 6$, we enumerate the sub-quads such that the superscript $1, 1$ corresponds to the corner point. Here $a : b$ denotes the sequence $a, a+1, \ldots, b$ if $a \le b$ and the sequence $a, a-1, \ldots, b$ if $a > b$. We will interpret the vertices of quad-layout as *B-spline-like control points* and obtain a grid-like refinement by uniform binary bi-3 B-spline subdivision. Then the level ℓ can be chosen to provide sufficient flexibility for modeling. We associate one polynomial patch $\mathbb{c}^{\alpha;kl}$ with each sub-quad (k, l) of a quad α and can represent them in tensor-product Bernstein-Bézier (BB) form of bi-degree $d = 3$,

$$\mathbb{c}(u, v) := \sum_{i=0}^{d} \sum_{j=0}^{d} \mathbb{c}_{ij} B_i^d(u) B_j^d(v), \quad (u, v) \in \square := [0..1]^2, \quad (1)$$

where $B_k^d(t) := \binom{d}{k}(1-t)^{d-k} t^k$ is the kth Bernstein-Bézier polynomial of degree d and $\mathbb{c}_{ij}$ are its BB-coefficients. That is, the BB-coefficients of each (tensor-product) patch of bi-degree d are denoted

$$\mathbb{c}_{ij}^{\alpha;kl}, \quad i, j \in 0 : d. \quad (2)$$

4. A hierarchy of G^1 spline surfaces on subdivided input meshes

Section 4.1 develops the G^1 constraints suitable for rational linear reparameterization. In particular, the partial derivatives of any two abutting patches are linearly related. Section 4.2 then gives a concrete algorithm for enforcing the constraints. This construction completes the proof of Lemma 1 where the claim was that any 3-6 polyhedron and hence any restricted polyhedron can be endowed with a smooth surface that satisfies the constraints of the restricted patch layout.

4.1. *A G^1 construction linearly relating partial derivatives*

The following lemma motivates the algorithm below by defining the G^1 continuity with linear reparameterization that the surface construction has to satisfy for an $n-n$ edge as well as the constant reparameterization for 3-6 edges.

Lemma 2. *Let* $\mathbf{p}^k := \mathbb{c}^{\alpha,k1}$ *and* $\mathbf{q}^k := \mathbb{c}^{\beta,1k}$ *be two patches (with coefficients* $\mathbf{p}_{ij}^k$ *and* $\mathbf{q}_{ij}^k$*) of degree bi-3 that share the boundary curve* $\mathbf{p}^k(t, 0) = \mathbf{q}^k(0, t)$*. For scalars* ω_0 *and* ω_1*, define*

$$\boldsymbol{\rho}^{\alpha;k}(\omega_0, \omega_1) := \frac{1}{3}(2\omega_0 \mathbf{p}_{20}^k - \omega_1 \mathbf{p}_{00}^k + (6 - 2\omega_0 + \omega_1)\mathbf{p}_{10}^k)$$
$$\boldsymbol{\sigma}^{\alpha;k}(\omega_0, \omega_1) := \frac{1}{3}(\omega_0 \mathbf{p}_{30}^k - 2\omega_1 \mathbf{p}_{10}^k + (6 - \omega_0 + 2\omega_1)\mathbf{p}_{20}^k)$$

Then $\mathbf{p}^k$ *and* $\mathbf{q}^k$ *join* G^1 *according to*

$$((1-t)\omega_0 + t\omega_1)(\partial_1 \mathbf{p}^k)(t, 0) = (\partial_2 \mathbf{p}^k)(t, 0) + (\partial_1 \mathbf{q}^k)(0, t) \quad \text{(G1)}$$

if and only if

$$\mathbf{p}_{01}^k + \mathbf{q}_{10}^k = \omega_0 \mathbf{p}_{10}^k + (2 - \omega_0)\mathbf{p}_{00}^k, \quad (3)$$
$$\mathbf{p}_{11}^k + \mathbf{q}_{11}^k = \boldsymbol{\rho}^{\alpha;k}(\omega_0, \omega_1), \quad (4)$$
$$\mathbf{p}_{21}^k + \mathbf{q}_{12}^k = \boldsymbol{\sigma}^{\alpha;k}(\omega_0, \omega_1), \quad (5)$$
$$\mathbf{p}_{31}^k + \mathbf{q}_{13}^k = (2 + \omega_1)\mathbf{p}_{30}^k - \omega_1 \mathbf{p}_{20}^k. \quad (6)$$

Proof Equation (G1) is equivalent to matching four BB-coefficients. Equations (3) and (6) enforce (G1) at $t = 0$ and $t = 1$, respectively. To verify the remaining observe that the four coefficients of $((1-t)\omega_0 + t\omega_1)(\partial_1 \mathbf{p}^k)(t, 0)$ are

$$\omega_0(\mathbf{p}_{10} - \mathbf{p}_{00}), \quad 2\omega_0(\mathbf{p}_{20} - \mathbf{p}_{10}) + \omega_1(\mathbf{p}_{10} - \mathbf{p}_{00}), \quad (7)$$
$$\omega_0(\mathbf{p}_{30} - \mathbf{p}_{20}) + 2\omega_1(\mathbf{p}_{20} - \mathbf{p}_{10}), \quad \omega_1(\mathbf{p}_{30} - \mathbf{p}_{20}) \quad (8)$$

and the coefficients of $(\partial_2 \mathbf{q})(0, t) + (\partial_1 \mathbf{p})(t, 0)$ are

$$\mathbf{p}_{01} + \mathbf{q}_{10} - 2\mathbf{p}_{00}, \quad 3(\mathbf{p}_{11} + \mathbf{q}_{11} - 2\mathbf{p}_{10}), \quad (9)$$
$$3(\mathbf{p}_{21} + \mathbf{q}_{12} - 2\mathbf{p}_{20}), \quad \mathbf{p}_{31} + \mathbf{q}_{13} - 2\mathbf{p}_{30}. \quad (10)$$

|||

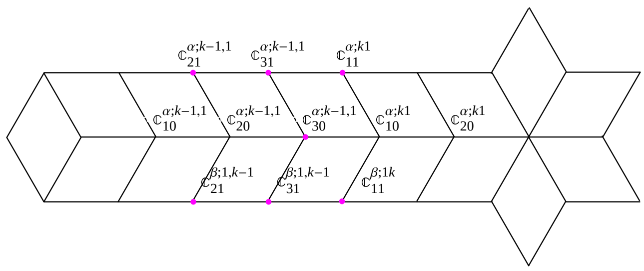

Figure 8: Indices of BB-coefficients along a 3-6 edge. Lemma 3 C^1 patch interior along $\mathbb{c}_{31}^{\alpha;k-1,1}$ $\mathbb{c}_{30}^{\alpha;k-1,1}$ and $\mathbb{c}_{30}^{\alpha;k-1,1}$ $\mathbb{c}_{31}^{\beta;1,k-1}$

Remarkably, to insure that $\mathbb{c}^{\alpha;k-1,1}$ and $\mathbb{c}^{\alpha;k,1}$ join C^1, for 3-6 edges it is necessary that the boundary curve itself be C^2. For 6-6 edges and 3-3 edges, no such constraint is needed as the following shows.

Lemma 3. *(see Fig. 8 for the indexing) Let* $\mathbb{c}^{\alpha;k-1,1}$ *and* $\mathbb{c}^{\beta;1,k-1}$ *join* G^1 *according to (G1) and* $\mathbb{c}^{\alpha;k1}$ *and* $\mathbb{c}^{\beta;1k}$ *join* G^1 *according to (G1). Then both* $\mathbb{c}^{\alpha;k-1,1}$ *and* $\mathbb{c}^{\alpha;k1}$ *join* C^1 *up to first order and* $\mathbb{c}^{\beta;1,k-1}$ *and* $\mathbb{c}^{\beta;1k}$ *join* C^1 *up to first order if and only if*

$$\begin{aligned}\mathbb{c}_{31}^{\alpha;k-1,1} &= (\mathbb{c}_{21}^{\alpha;k-1,1} + \mathbb{c}_{11}^{\alpha;k1})/2,\\ \mathbb{c}_{31}^{\beta;1,k-1} &= (\mathbb{c}_{21}^{\beta;1,k-1} + \mathbb{c}_{11}^{\beta;1k})/2,\end{aligned} \tag{11}$$

and

$$(\omega_0^{k-1} + \omega_1^k)(-\mathbb{c}_{10}^{\alpha;k-1,1} + 2\mathbb{c}_{20}^{\alpha;k-1,1} - 2\mathbb{c}_{10}^{\alpha;k1} + \mathbb{c}_{20}^{\alpha;k,1}) = 0. \tag{12}$$

Proof Setting $\mathbb{c}_{31}^{\alpha;k-1,1}$ and $\mathbb{c}_{31}^{\beta;1,k-1}$ according to (11) enforces the C^1 constraints away from the central point shared by all four patches. Symbolically solving the four G^1-constraints of type (5) and (6) for $\mathbb{c}^{\alpha;k-1}$ and $\mathbb{c}^{\beta;k-1}$, respectively (3) and (4) for $\mathbb{c}^{\alpha;k}$ and $\mathbb{c}^{\beta;k}$, then enforces $\mathbb{c}_{30}^{\alpha;1,k-1} = (\mathbb{c}_{20}^{\beta;1,k-1} + \mathbb{c}_{10}^{\beta;1k})/2$ if and only if (12) holds. Here we use that, in (G1), $\omega_1^{k-1} = \omega_0^k = (\omega_0^{k-1} + \omega_1^k)/2$ due to the rational linear reparameterization. |||

We note that when the boundary is of type 6-6 or 3-3 and $k = 2^\ell/2$ (the midpoint of the curve) then our construction will automatically yield $\omega_0^{k-1} + \omega_1^k = 0$ and the first factor of (12) vanishes. If the edge is of type 3-6, we can divide the expression in (12) by $(\omega_0^{k-1} + \omega_1^k) \neq 0$ and obtain the constraint that the pieces of $\gamma(t)$ must be C^2 connected since it represents the difference of two second differences at their common point.

4.2. Algorithm: construct a smooth, piecewise bi-3 surface from a restricted polyhedron

We now state in detail the algorithm that enforces Lemma 2 and Lemma 3.

Input: An ℓ-times binarily subdivided 3-6 polyhedron of genus g.

Output: A surface of genus g consisting of bi-cubic tensor-product spline surfaces $\mathbb{c}^\alpha$ that join either C^2, C^1 (across 3-6 edges) or G^1 (across 3-3 edges and 6-6 edges).

Initialization: We interpret all input mesh points as bi-3 B-spline control points and, where possible, convert from B-spline to BB-form to initialize all BB-coefficients $\mathbb{c}_{ij}^{\alpha;kl}$. This leaves only the points with label $\mathbb{c}_{00}^{\alpha;11}$ uninitialized, corresponding to the non-4-valent corners.

Overview: Consider the

$$G^1 \textit{ strip} \text{ of BB-coefficients } \quad \mathbb{c}_{ij}^{\alpha;k1}, \mathbb{c}_{ij}^{\beta;k1}, \quad i = 0,1, j = 0,1,2,3, \quad k = 1 : 2^\ell$$

involved in the G^1 join between two 3-6 quads $\mathbb{c}^\alpha$ and $\mathbb{c}^\beta$, along a curve $\gamma(t)$. Visiting each patch $\mathbb{c}^{\alpha;k1}$, $\mathbb{c}^{\beta;k1}$, starting from each vertex of valence 6 to the middle index, $k = 1 : \mu_\ell := 2^{\ell-1} - 1$ half-ways to its neighbor of valence 3 or 6, we adjust the BB-coefficients of the G^1 strip. Then we move $k = \mu_\ell : 1$, from middle towards the vertices of valence 3 to adjust the remaining coefficients of the G^1 strip.

1. For vertices of valence $\mathbf{n} = \mathbf{6}$.
   (a) For $k = 1 : \mu_\ell$, i.e. up to the middle of the edge, set
   $$\begin{cases}\omega_0^k := 1 - \frac{2(k-1)}{2^\ell}, \quad \omega_1^k := 1 - \frac{2k}{2^\ell}, & \text{for a 6-6 edge,}\\ \omega_0^k := 1, \quad \omega_1^k := 1, & \text{for a 6-3 edge}\end{cases}$$
   (b) For all n patches α surrounding the vertex, apply the cosine projection matrix P to the tangent coefficients
   $$\mathbb{c}_{10}^{\alpha;11} \leftarrow P\mathbb{c}_{10}^{\alpha;11} \qquad P := (J + C)/n \in \mathbb{R}^{n\times n} \tag{13}$$
   $$J(i,j) := 1, \quad C(i,j) := 2\cos(\frac{2\pi}{n}(j-i)).$$
   (c) Set the vertex of valence $n = 6$ to the average
   $$\mathbb{c}_{00}^{\alpha;11} := \frac{1}{n}\sum_{\alpha=0}^{n-1} \mathbb{c}_{10}^{\alpha;11}. \tag{14}$$
   (d) Adjust the second derivatives of the ends of the boundary curves, and the mixed derivatives accordingly
   $$\mathbb{c}_{20}^{\alpha;11} \leftarrow \mathbb{c}_{20}^{\alpha;11} - \frac{(-1)^\alpha}{4}\mathbf{a}, \tag{15}$$
   $$\mathbf{a} := \sum_{\alpha=0}^{n-1}(-1)^\alpha R_\alpha, \quad R_\alpha := \frac{1}{2}\boldsymbol{\rho}^{\alpha;1}(\omega_0^1, \omega_1^1),$$
   $$\mathbb{c}_{11}^{\alpha;11} := \begin{bmatrix} 1&1&0&0&0&0\\ 0&1&1&0&0&0\\ 0&0&1&1&0&0\\ 0&0&0&1&1&0\\ 0&0&0&0&1&1\\ 1&0&0&0&0&1\end{bmatrix}^+ R. \tag{16}$$
   (e) For each 6-3 edge, make the curves C^2 up to the *middle of the edge*. For $k = 1 : \mu_\ell$
   $$\mathbb{c}_{10}^{\alpha;k+1,1} := \mathbb{c}_{20}^{\alpha;k1} + \frac{1}{2}(\mathbb{c}_{20}^{\alpha;k+1,1} - \mathbb{c}_{10}^{\alpha;k1}). \tag{17}$$
   (f) For $k = 1 : \mu_\ell$, i.e. up to the middle of the edge, minimally perturb the transversal derivatives to enforce G^1 continuity:
   $$\mathbb{c}_{11}^{\alpha;k1} \leftarrow \mathbb{c}_{11}^{\alpha;k1} + \frac{1}{2}(\boldsymbol{\rho}^{\alpha;k}(\omega_0^k, \omega_1^k) - \mathbb{c}_{11}^{\alpha;k1} - \mathbb{c}_{11}^{\beta;1k}), \tag{18}$$
   $$\mathbb{c}_{21}^{\alpha;k1} \leftarrow \mathbb{c}_{21}^{\alpha;k1} + \frac{1}{2}(\boldsymbol{\sigma}^{\alpha;k}(\omega_0^k, \omega_1^k) - \mathbb{c}_{11}^{\alpha;k1} - \mathbb{c}_{11}^{\beta;1k}),$$
   (g) For $k = 1 : \mu_\ell$ average up to the midpoint (to enforce C^1 continuity within the 3-6 quads α and the neighbor β of α):
   $$\begin{aligned}\mathbb{c}_{30}^{\alpha;k-1,1} &:= (\mathbb{c}_{20}^{\alpha;k-1,1} + \mathbb{c}_{10}^{\alpha;k1})/2,\\ \mathbb{c}_{31}^{\alpha;k-1,1} &:= (\mathbb{c}_{21}^{\alpha;k-1,1} + \mathbb{c}_{11}^{\alpha;k1})/2,\\ \mathbb{c}_{31}^{\beta;1,k-1} &:= (\mathbb{c}_{21}^{\beta;1,k-1} + \mathbb{c}_{11}^{\beta;1k})/2.\end{aligned} \tag{19}$$
2. For vertices of valence $\mathbf{n} = \mathbf{3}$.
   (a) For $k = 1 : \mu_\ell$
   $$\begin{cases}\omega_0^k := \frac{2(k-1)}{2^\ell} - 1, \quad \omega_1^k := \frac{2k}{2^\ell} - 1, & \text{for a 3-3 edge,}\\ \omega_0^k := -1, \quad \omega_1^k := -1, & \text{for a 3-6 edge.}\end{cases}$$

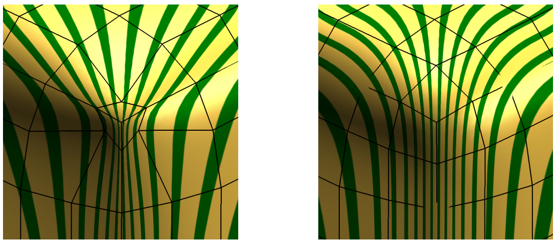

(a) without 2b; $\kappa = 0$ (b) with 2b: $\kappa = 1/2$

Figure 9: Scaling of tangent coefficients for $n = 3$

(b) For $n = 3$, the B-spline to BB-conversion pulls the tangent coefficients too close together to their average $\mathbb{c}_{00} := \frac{1}{3}\sum_{\alpha=0}^{2} \mathbb{c}_{10}^{\alpha;11}$ (see Fig. 9). For better shape, we overwrite them by

$$\mathbb{c}_{10}^{\alpha;k1} \leftarrow \mathbb{c}_{10}^{\alpha;k1} + \kappa(\mathbb{c}_{10}^{\alpha;k1} - \mathbb{c}_{00}), \qquad \kappa_{default} := 1/2.$$

(c) Set

$$\mathbb{c}_{00}^{\alpha;11} := \frac{1}{n}\sum_{\alpha=0}^{n-1} \mathbb{c}_{10}^{\alpha;11}, \tag{20}$$

(d) Adjust

$$\mathbb{c}_{11}^{\alpha;11} := \begin{bmatrix} 1 & 1 & 0 \\ 0 & 1 & 1 \\ 1 & 0 & 1 \end{bmatrix}^{-1} R, \quad R_\alpha := \rho^{\alpha;1}(\omega_0^1, \omega_1^1). \tag{21}$$

(e) For each 3-6 edge, starting from the midpoint, make the curves C^2. For $k = \mu_\ell : 1$ (note the ordering!)

$$\mathbb{c}_{20}^{\alpha;k1} := \mathbb{c}_{10}^{\alpha;k+1,1} - \frac{1}{2}(\mathbb{c}_{20}^{\alpha;k+1,1} - \mathbb{c}_{10}^{\alpha;k1}). \tag{22}$$

(f) For $k = 1 : \mu_\ell$, enforce (18) (i.e. minimally perturb the transversal derivatives). Due to the weights ω_0^k, ω_1^k this enforces C^1 continuity across the edge.

(g) For $k = 1 : \mu_\ell$, enforce (19). Due to the weights ω_0^k, ω_1^k this enforces C^1 continuity of the patches to either side.

This completes the algorithm. We note that pairs of tensor-product spline patches joining across a 3-6 edge are parametrically C^1 connected. To obtain still better shape, one might optimize the B-spline control points and hence BB-coefficients away from the G^1 strips. However, this is not our focus here.

4.3. Examples

The vertices of the subdivided 3-6 polyhedron serve as the control points and degrees of freedom of the surface construction. It is convenient to tabulate the function associated with each type of vertex so that we can use the vertices as B-spline-like control points of the surface. Fig. 10 shows the layout and the detailed BB-coefficient structure on our so-constructed genus $g = 5$ cube-like shape. More detailed modelling can start with a (typically once-refined) 3-6 polyhedron and adding geometric detail by increasing the tensor-product refinement level ℓ as in Fig. 11 and thus generating more B-spline-like control points. In general, once the 3-6 polyhedron-structure is chosen, it is possible to pack much of the geometric detail into the regular tensor-product spline interior of each 3-6 quad and make the vertices of valence $n = 3$, $n = 6$ less prominent.

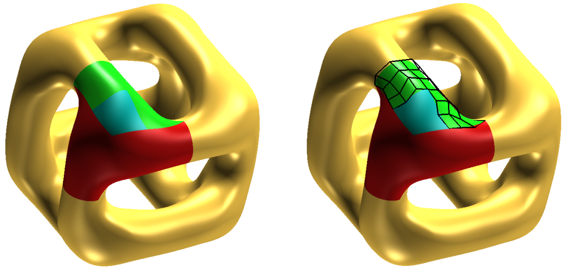

(a) Level 1

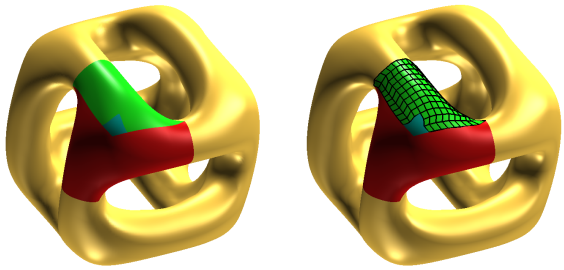

(b) Level 2

Figure 10: Genus 5 surface (built from [3,6,6,6] 3-6 quads) parameterized at two levels. The right display shows the BB-net superimposed and indicates the size of the polynomial pieces of the 48 spline patches.

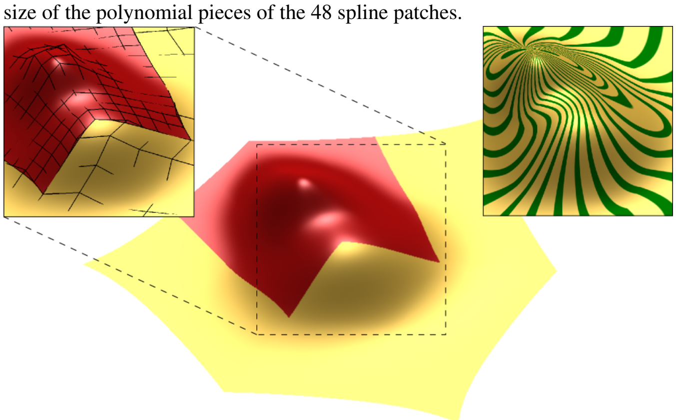

Figure 11: Combining level $\ell = 1$ and $\ell = 2$ along a 3-6 edge. The result is again smooth as the highlight lines in the lower right enlargement indicate.

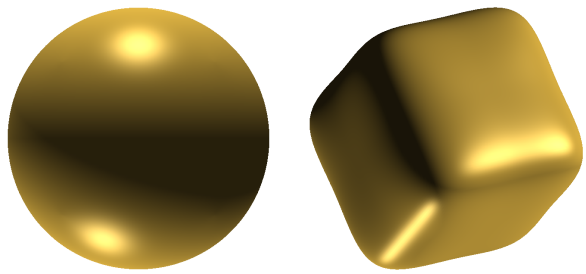

(a) [3,3,3,3] quads only

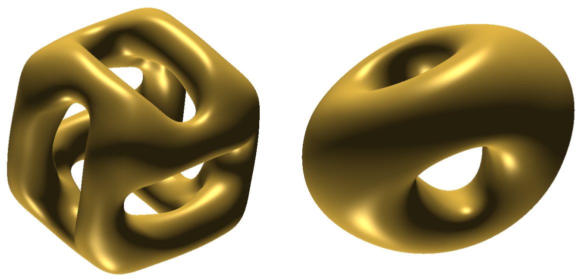

(b) [3,6,6,6] quads only

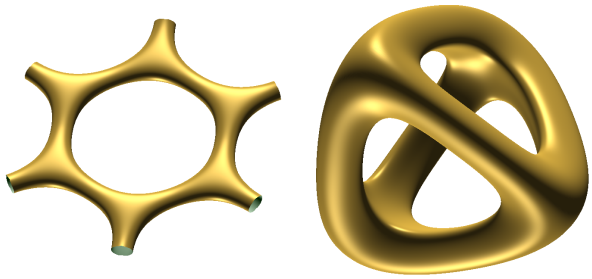

(c) [6,6,6,6] quads only

Figure 12: Gallery of polynomial spline surfaces with rational linear transitions built from different symmetrically-arranged families of 3-6 quads and with different pants geometry. (The models are illuminated by two white point light sources).

5. Conclusion

Since valence $n = 3$ vertices can be employed to model convex configurations and valence $n = 6$ to model saddle points, the new class of polynomial spline surfaces allow a wide range of designs, certainly compared to the valence 8 quads in [PF10]. Vertices of valence higher than $n = 6$ can be split to decrease their valence, but 3-6 polyhedra do lack vertices of valence $n = 5$. Fig. 12 shows a set of models that include sphere-like and cube-like shapes of genus 0, with all 3-3 edges, and higher-genus objects assembled form pairs of pants. Torus-like shapes are trivially modelled by tensor-product splines.

Valences 3 and 6 form the only *pair* of valences satisfying the restricted patch layout of Definition 1 for quad meshes and structurally symmetric constructions. The pair is special in that the opening angle formed by the tangent configurations are complementary: only for this pair can the weight $\omega(t)$ in the G1 constraints be constant when the neighboring vertices have differing valences. (The weight equals $\pm 1 = \cos(2\pi/n)$, $n \in \{3, 6\}$ with the sign depending on the direction of the differentiation.)

Given the importance of 'pairs of pants' in topological geometry and hyperbolic geometry, the concrete parameterizations with minimal transition maps may be useful beyond shape modelling. This and the connection to rational constructions based on projections from homogeneous space need to be explored further.

ACKNOWLEDGMENTS

Work supported by the National Science Foundation under grant CCF-1117695. We thank Hartmut Prautzsch and Ergun Akleman for their interest and their interpretation of the work.

[Akl14] Ergun Akleman. Topmod constructions, Nov 2014. Personal Communication.

[ANS96] Peter Alfeld, Marian Neamtu, and Larry L. Schumaker. Bernstein–Bézier polynomials on spheres and sphere-like surfaces. *Computer Aided Geometric Design*, 13(4):333–349, 1996.

[BGN14] C Beccari, D Gonsor, and M Neamtu. Rags: Rational geometric splines for surfaces of arbitrary topology. *Computer Aided Geometric Design*, 31:97110, 2014.

[EG79] Murray Eisenberg and Robert Guy. A proof of the hairy ball theorem. *The American Mathematical Monthly*, 86(7):571574, 1979.

[GH95] Cindy M. Grimm and John F. Hughes. Modeling surfaces of arbitrary topology using manifolds. In *Proceedings of the 22Nd Annual Conference on Computer Graphics and Interactive Techniques*, SIGGRAPH '95, pages 359–368, New York, NY, USA, 1995. ACM.

[HXA+12] Shiyu Hu, Qing Xing, Ergun Akleman, Jianer Chen, and Jonathan L. Gross. Pattern mapping with quad-pattern-coverable quad-meshes. *Computers & Graphics*, 36(5):455–465, 2012.

[Mil58] J. W. Milnor. On the existence of a connection with curvature zero. *Comm. Math. Helv.*, 32(1):215223, 1958.

[Mir08] Maryam Mirzakhani. Growth of the number of simple closed geodesics on hyperbolic surfaces. *Ann. of Math. (2)*, 168(1):97–125, 2008.

[Möb46] August Ferdinand Möbius. Ueber eine neue Behandlungsweise der analytischen Sph"arik. *Abhandlungen bei Begründung der Königl.Sächs.Gesellschaft der Wissenschaften*, pages 45–86, 1846. In: Werke, Bd.2, S. 1–54.

[PF09] J. Peters and Jianhua Fan. On the complexity of smooth spline surfaces from quad meshes. *Computer Aided Geometric Design*, 27:96–105, 2009.

[PF10] Jörg Peters and Jianhua Fan. The projective linear transition map for constructing smooth surfaces. In jean philippe.pernot, editor, *Shape Modelling International, SMI10 conference*, pages 124–130. IEEE Computer Society, June 21-23 2010.

[VJK08] Giovanni Della Vecchia, Bert Jüttler, and Myung-Soo Kim. A construction of rational manifold surfaces of arbitrary topology and smoothness from triangular meshes. *Computer Aided Geometric Design*, 25(9):801–815, 2008.

[WP98] Johannes Wallner and Helmut Pottmann. Spline orbifolds. In A. Le Méhauté, C. Rabut, and L. L. Schumaker, editors, *Curves and Surfaces with Applications in CAGD*, pages 445–464, 1998.

[YZ04] Lexing Ying and Denis Zorin. A simple manifold-based construction of surfaces of arbitrary smoothness. *ACM Trans. Graph*, 23(3):271–275, 2004.